

A virtual rat for simulating environmental and exertional heat stress

Vineet Rakesh, Jonathan D. Stallings and Jaques Reifman

J Appl Physiol 117:1278-1286, 2014. First published 2 October 2014;

doi:10.1152/jappphysiol.00614.2014

You might find this additional info useful...

This article cites 28 articles, 9 of which can be accessed free at:

</content/117/11/1278.full.html#ref-list-1>

Updated information and services including high resolution figures, can be found at:

</content/117/11/1278.full.html>

Additional material and information about *Journal of Applied Physiology* can be found at:

<http://www.the-aps.org/publications/jappl>

This information is current as of December 19, 2014.

A virtual rat for simulating environmental and exertional heat stress

Vineet Rakesh,¹  Jonathan D. Stallings,² and Jaques Reifman¹

¹Department of Defense Biotechnology High Performance Computing Software Applications Institute, Telemedicine and Advanced Technology Research Center, United States Army Medical Research and Materiel Command, Fort Detrick, Maryland; and ²Environmental Health Program, United States Army Center for Environmental Health Research, Fort Detrick, Maryland

Submitted 8 July 2014; accepted in final form 18 September 2014

Rakesh V, Stallings JD, Reifman J. A virtual rat for simulating environmental and exertional heat stress. *J Appl Physiol* 117: 1278–1286, 2014. First published October 2, 2014; doi:10.1152/jappphysiol.00614.2014.— Severe cases of environmental or exertional heat stress can lead to varying degrees of organ dysfunction. To understand heat-injury progression and develop efficient management and mitigation strategies, it is critical to determine the thermal response in susceptible organs under different heat-stress conditions. To this end, we used our previously published virtual rat, which is capable of computing the spatiotemporal temperature distribution in the animal, and extended it to simulate various heat-stress scenarios, including 1) different environmental conditions, 2) exertional heat stress, 3) circadian rhythm effect on the thermal response, and 4) whole body cooling. Our predictions were consistent with published in vivo temperature measurements for all cases, validating our simulations. We observed a differential thermal response in the organs, with the liver experiencing the highest temperatures for all environmental and exertional heat-stress cases. For every 3°C rise in the external temperature from 40 to 46°C, core and organ temperatures increased by ~0.8°C. Core temperatures increased by 2.6 and 4.1°C for increases in exercise intensity from rest to 75 and 100% of maximal O₂ consumption, respectively. We also found differences as large as 0.8°C in organ temperatures for the same heat stress induced at different times during the day. Even after whole body cooling at a relatively low external temperature (1°C for 20 min), average organ temperatures were still elevated by 2.3 to 2.5°C compared with normothermia. These results can be used to optimize experimental protocol designs, reduce the amount of animal experimentation, and design and test improved heat-stress prevention and management strategies.

three-dimensional computational rat model; heat transfer; core temperature circadian rhythm; organ-specific response; whole body cooling

EXPOSURE TO ADVERSE ENVIRONMENTAL conditions, strenuous exercise, or their combination may lead to heat stress, which characteristically involves an increase in body temperatures (8). Environmental, or classical, heat stress is caused by exposure to high external temperatures and is predominantly observed in very young or elderly people or in those who are unable to escape prolonged exposure to high external temperatures (3). Exertional heat stress is common in service members and athletes who perform strenuous physical activity under hot, warm, or even relatively cool environmental conditions (1, 2, 5).

Experimental animal models are frequently used to study heat-injury progression (3, 17) resulting from both environ-

mental and exertional heat-stress conditions (7). With both of these conditions having been reported to lead to varying degrees of organ dysfunction, such as encephalopathy, myocardial injury, and hepatocellular injury (3, 18), it is critical to accurately determine the initial organ-specific thermal insult so as to delineate the progression of these disorders. Rats are often the preferred animal model used in heat-stress experiments, as they are readily available, cost-effective, and convenient to handle, and they demonstrate certain similarities to humans during thermoregulation (7, 11). Several studies have used experimental rat models to investigate environmental and exertional heat stress (9, 19, 27, 29), whole body cooling strategies to manage heat stress (29), and circadian rhythms during thermoregulation (22, 25). However, due to their inability to measure the spatiotemporal temperature distribution in vivo throughout the animal, such experimental studies have provided limited insights about the thermal load in specific organs. Moreover, with the use of experimental animal models alone, it is difficult to decouple the effects of exertional heat stress when those are confounded by adverse environmental conditions (16).

Computational modeling used in conjunction with experimental animal models can provide an effective recourse to address these limitations. Several computational rat and mouse models have been reported in the literature; however, simplifying modeling assumptions, such as simple, anatomically unrealistic geometry (12), constant blood temperature (26), no heat transfer due to blood perfusion (23), and no circadian variations (13), make them unsuitable for accurately determining the spatiotemporal temperature distribution in the animal due to heat stress and for performing mechanistic analysis. We have previously presented a detailed anatomically and physiologically realistic virtual rat and demonstrated its ability to compute the spatiotemporal temperature distribution in the animal for one specific heat-stress protocol (21). Here, we use the virtual rat to simulate numerous previously reported experimental protocols, including a combination of environmental heat stress, exertional heat stress, whole body cooling, and circadian variations (7, 12, 16, 21, 22, 28). In addition to providing valuable new information to study heat stress without the need for performing additional experiments, the virtual rat facilitates the design of focused experiments and can be used as a unifying framework for comparing observations from different experimental studies and for simulating additional heat-stress conditions not included in the original experiments.

Accordingly, we followed a systematic approach to investigate the various aspects of heat stress. First, we reviewed the literature for representative experimental protocols of heat-stress conditions that we intended to investigate. Next, we used the experimental protocol conditions as input parameters to the

Address for reprint requests and other correspondence: J. Reifman, Dept. of Defense Biotechnology High Performance Computing Software Applications Institute, Telemedicine and Advanced Technology Research Center, U.S. Army Medical Research and Materiel Command, MCMR-TT, 504 Scott St., Fort Detrick, MD 21702-5012 (e-mail: jaques.reifman.civ@mail.mil).

computational model to exactly mimic the experiment in the virtual rat. Subsequently, we compared our predictions with the experimental data to validate our simulations for each protocol. We did not use the compared data as input parameters for the simulations or to fit the model. Next, we analyzed the simulation results, such as the spatial temperature distribution in the animal's body and organs, which were not possible in the original experiments. Finally, we performed additional simulations using the virtual rat to facilitate comparative analysis of the thermal response for various relevant conditions and gain deeper insights into critical aspects of heat stress.

MATERIALS AND METHODS

We previously developed a three-dimensional computational rat model, i.e., a “virtual rat,” to simulate the thermal response in the animal due to heat stress (21). Figure 1 shows an overview of the model, which takes the environmental and exertional conditions as inputs and computes the spatiotemporal temperature distribution in the animal. The model itself includes an anatomically realistic description of the animal obtained from medical imaging and incorporates the various heat transfer mechanisms involved during thermoregulation (Fig. 1). We used the Pennes bioheat transfer equation (20, 28) to formulate the mathematical model. To describe heat transfer within the body of the animal, we modeled heat conduction, heat convection due to blood perfusion, heat generation due to metabolism and physical activity, and heat loss due to intake of water at a temperature lower than the body. We also accounted for circadian rhythms in blood perfusion and metabolic heat generation. To describe the heat transfer of the animal with the surroundings, we included convection, radiation, and evaporative cooling. Additional details regarding the development of the virtual rat are included in our previous work (21).

We performed model simulations that replicated various experimental protocols reported in the literature to investigate scenarios that lead to heat stress and to manage it: 1) different environmental conditions, 2) different exertional conditions, and 3) whole body cooling. In addition, we investigated the effect of circadian rhythms on the thermal response by simulating animal heat-stress exposure at different times during the day. We obtained input parameters for the simulations from the published experiments and validated the virtual rat predictions by comparing them with experimentally measured temperatures in the animal. The details of the heat-stress conditions and input parameters used for the simulations and model validation are provided in RESULTS.

We simulated environmental heat stress by specifying the external temperature and duration of exposure as boundary conditions to the model. Similarly, we simulated whole body cooling by specifying the external cooling temperature and cooling time as boundary conditions. To simulate exertional heat stress, we used the value of exercise intensity, calculated based on the running speed of the animal, to modulate the metabolic heat generation term in the Pennes bioheat transfer equation (20). First, we calculated the $\dot{V}O_2$ consumption for a particular running speed (v_{run}) based on the following relationship developed by Patch and Brooks (19) for rats:

$$\dot{V}O_2 = \begin{cases} 0.664v_{run} + 41.69 & \text{for untrained rats} \\ 0.647v_{run} + 46.04 & \text{for trained rats} \end{cases} \quad (1)$$

where $\dot{V}O_2$ is expressed in milliliters per kilogram per minute and v_{run} is expressed in meters per minute. Next, we determined exercise intensity by calculating the ratio of $\dot{V}O_2$ for the corresponding running speed to the $\dot{V}O_2$ at rest, also reported by Patch and Brooks (19). Finally, we used this ratio to modulate the metabolic heat generation term for incorporating exertional heat stress. We previously demonstrated the effects of circadian rhythms on core temperature in the simulation of one specific experimental protocol (21). Here, we performed additional simulations to investigate the differential thermal responses exhibited by animals exposed to the same heat-stress conditions at different times during the day. We used a commercial finite-element solver, COMSOL Multiphysics (COMSOL, Burlington, MA), to perform the computations.

RESULTS

Environmental heat stress under different external conditions. In the first set of simulations, we investigated the effects of different external temperatures on the animal's thermal response, using the protocol proposed by Yang et al. (29). The animals were exposed to an external temperature of 43°C for 49 min and were subsequently allowed to recover at 26°C (Fig. 2A). We performed simulations of these conditions using the virtual rat. Figure 2B shows the comparison between the simulation predictions and the measured core temperature over the 120 min of the experimental protocol (29). Our results closely matched the experimental data, yielding a very similar core-temperature profile with a maximum temperature increase of 6.0°C. Comparing the spatial temperature distribution before heat exposure (time = 0 min) to that immediately after removal from the external heating (time = 94 min), we

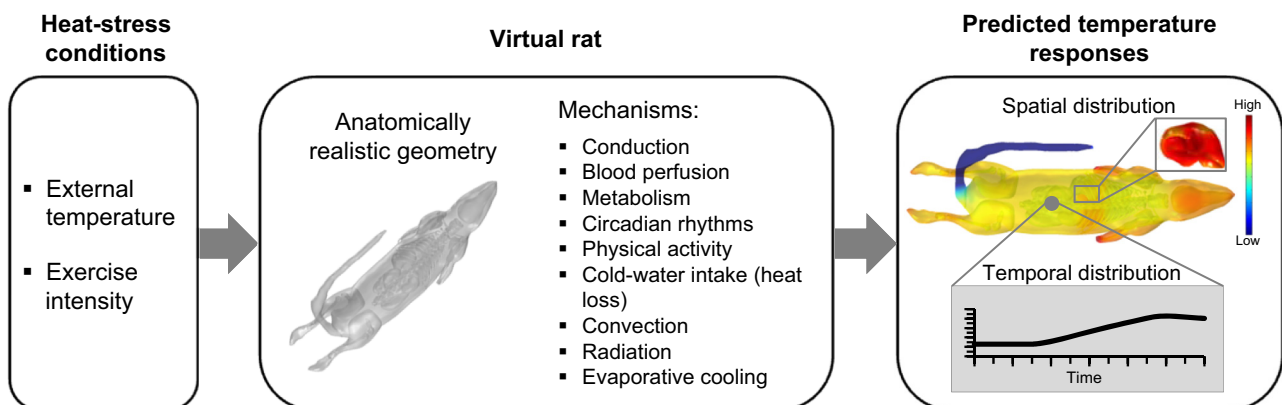
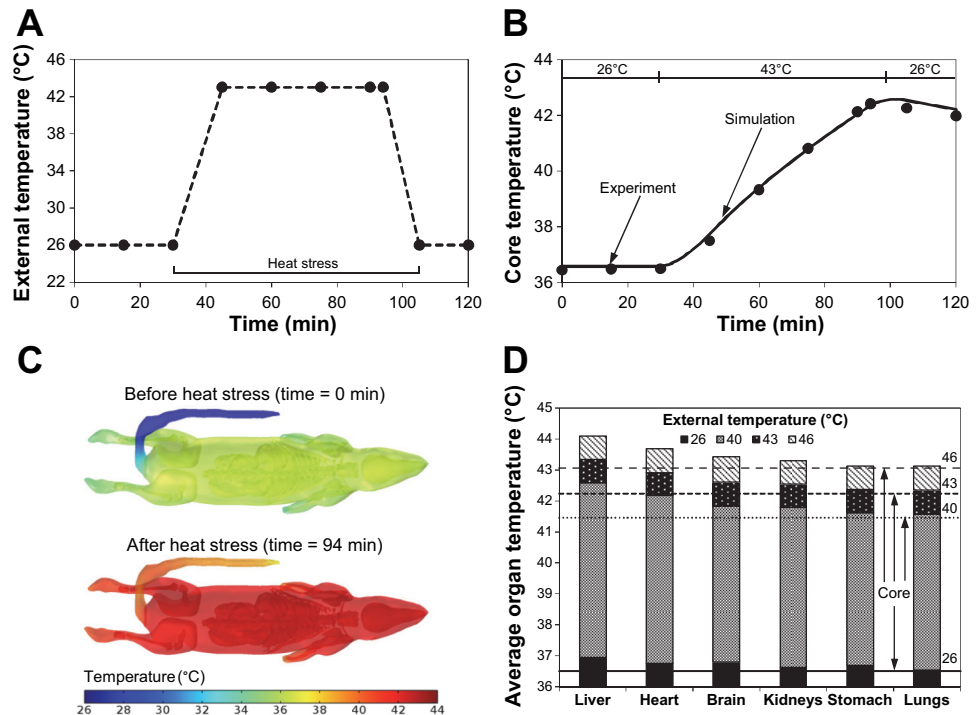


Fig. 1. Illustration of the virtual rat. The model includes an anatomically realistic description of the rat obtained from medical imaging and incorporates the major heat transfer mechanisms involved during thermoregulation (see Ref. 21). We extended the model to include the effect of exercise on the thermal response. The model takes the external temperature and exercise intensity as inputs and computes the spatiotemporal temperature distribution in the animal.

Fig. 2. Thermal response due to increase in environmental temperature based on the protocol used in Ref. 29. In the experimental study, adult male Sprague-Dawley rats ($n = 8$) weighing 238–312 g were housed in cages for ≥ 1 wk to acclimatize at an ambient temperature of $22 \pm 1^\circ\text{C}$, with a 12:12-h light-dark cycle, before undergoing the heat-stress protocol. Core temperature was measured using a thermocouple (DR130; Yokogawa, Yamanashi-ken, Japan) inserted into the rectum. *A*: external temperature profile used to induce heat stress. *B*: comparison of simulation predictions and experimentally measured ($n = 8$) core temperature. The dots (experimental data) represent the average values (standard errors were negligible). *C*: predicted spatial temperature distribution before (time = 0) and after heat stress (time = 94 min). *D*: predicted volume-averaged temperatures in the major organs (bars) and core temperatures (lines) at time = 94 min for exposure to external temperatures of 26 (normal room temperature), 40, 43, and 46°C. Organ temperatures are shown as incremental values across the increasing external temperatures for clarity.



observed an overall temperature increase throughout the body of the animal, with the temperature rise being more pronounced in the tail (Fig. 2C). In fact, while the core temperature rose by 6.0°C , the average tail temperature increased by 15.0°C .

To study the organ-specific thermal response to this heat-stress condition, we calculated the volume-averaged temperature (referred to as “average temperature” henceforth) in various organs from the model predictions and compared them with the temperature at the core. We also performed simulations with external temperatures of 40 and 46°C to investigate the organ-specific heat-stress response in different environmental conditions. Figure 2D shows the average organ temperatures at a room temperature of 26°C and at external temperatures of 40, 43, and 46°C immediately after removal from heat stress at 94 min. To facilitate comparisons between core and organ temperatures, we plotted the predicted core temperatures of the rat for the different environmental conditions and observed that the average organ temperatures were generally higher than the core temperature. The liver consistently attained the highest temperatures, on average $\sim 1.1^\circ\text{C}$ higher than the core temperature across the different environmental conditions, while heart and brain temperatures averaged ~ 0.7 and $\sim 0.4^\circ\text{C}$ higher than the core, respectively. Average temperatures in other organs, including the kidneys, stomach, and lungs, were (on average) within $\sim 0.3^\circ\text{C}$ of the core temperature. Compared across different environmental conditions, we observed that for every 3°C rise in the external temperature from 40 to 46°C , the core and organ temperatures increased by $\sim 0.8^\circ\text{C}$.

To demonstrate the capability of the virtual rat to replicate different heat-stress scenarios, we simulated the intraperitoneal heating protocol proposed by Shido and Nagasaka (24), where they heated rats using an electrical heater implanted in the peritoneal cavity for 30 min and reported the brain temperature

response. We simulated the heat load of 6.5 W/kg applied in the experimental protocol as a source term in the virtual rat and noted that the predicted brain temperature after 30 min was within 0.2°C of the measured value with a coefficient of determination (R^2) of 0.88.

Exertional heat stress under different environmental conditions. To study exertional heat stress, we used the protocol investigated by Fuller et al. (9), where they monitored brain and abdominal temperatures in rats exercising under different environmental conditions. Each animal was subjected to three sets of different experimental conditions, where in each condition the animal ran until fatigued on a treadmill moving at 15 m/min, corresponding to an exercise intensity of 68% of maximal $\dot{V}\text{O}_2$ ($\dot{V}\text{O}_{2\text{max}}$; calculated using Eq. 1 for trained rats). In the first set of experiments (*condition I* in Fig. 3A), each rat initially rested for 30 min at an external temperature of 23°C . Next, the external temperature was increased to 33°C , and the rats were forced to run on the treadmill until fatigued (~ 32 min). For the second set of experiments (*condition II* in Fig. 3B), rats rested for 30 min at 23°C before exercising in the treadmill until fatigued (~ 27 min) at an external temperature of 38°C . In the third set of experiments (*condition III* in Fig. 3C), rats first rested (~ 30 min) and then exercised (~ 17 min) at the same external temperature of 38°C . For each condition, the animals were kept at the same external exercise temperature for an additional 3 min after the termination of the exercise and then exposed to an external temperature of 23°C to cool down. We used these three exercise conditions to simulate exertional heat stress using the virtual rat.

Figure 3A shows the predicted brain temperatures as a function of time compared with the experimental measurements in one rat (as reported in Ref. 9) for *condition I*. The simulation accurately captured the magnitude and timing of the temperature increase in the brain, as well as the subsequent decrease in temperature during rest at a cooler external tem-

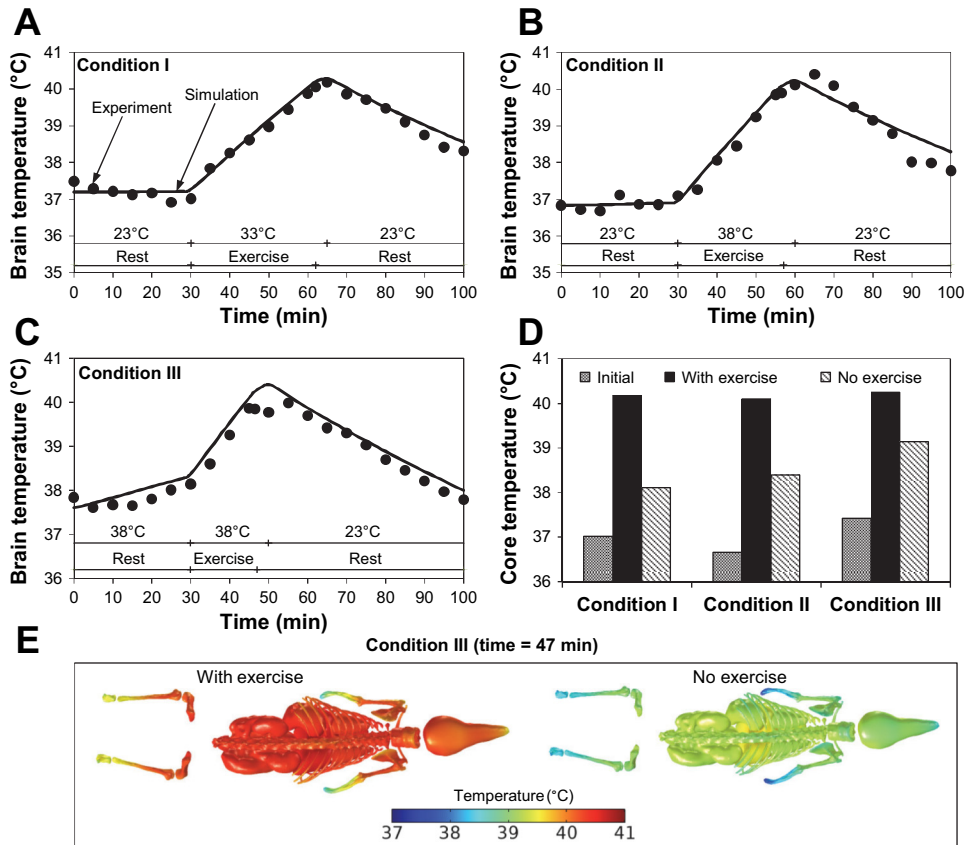


Fig. 3. Simulation of exertional heat stress in rats exercising at the same intensity under 3 different external temperature conditions based on the protocol used in Ref. 9. In the experimental study, 24 male Sprague-Dawley rats, raised and housed in cages at an ambient temperature of 22–23°C, with a 12:12-h light-dark cycle, underwent a 6-wk progressive endurance-training program. Each of the eight rats (weighing 350–450 g) that successfully completed the training was subjected to the 3 heat-stress conditions. Brain temperatures were measured using surgically implanted thermocouples (with an accuracy of $\pm 0.05^\circ\text{C}$) connected to a data-acquisition unit (3421A; Hewlett-Packard, Santa Clara, CA). Experimental data (9) were reported for only 1 representative rat. *A–C*: comparison of the simulated brain temperature profile with experimental data for a rat subjected to 3 experimental conditions. *D*: comparisons of simulated core temperatures with and without exercise for the same external temperatures as in the 3 conditions. *E*: simulated spatial temperature distributions for *condition III*.

perature, with values similar to those observed in the experiments. The rise in brain temperature predicted by the simulation was 3.1°C compared with the experimentally measured temperature increase of 3.2°C . During the cooling phase, the predicted decrease in brain temperature was 1.7°C compared with 1.9°C observed in the experiment. Similarly, the simulations were able to predict the thermal response in the brain for *conditions II* and *III* (Fig. 3, *B* and *C*, respectively) reasonably well ($R^2 = 0.95$ and 0.90 for *conditions II* and *III*, respectively). The predicted abdominal temperatures also closely matched the measured data ($R^2 = 0.95$, 0.94 , and 0.83 for *conditions I*, *II*, and *III*, respectively; results not shown). Although the exercise intensity was the same (68% of $\dot{V}O_{2\max}$) in *conditions I* and *II*, the rate of brain-temperature increase given by the slope of the temperature curve was faster for *condition II* than *condition I*. This was expected, because the rat exercised at a higher external temperature in *condition II* compared with *condition I* (38 vs. 33°C), which was accurately captured in the simulation. For *condition III*, we observed a noticeable increase in the brain temperature during the initial resting phase, which was captured in our simulation. Again, this was expected, because the rat was exposed to a higher external temperature of 38°C in contrast with *conditions I* and *II*, in which the external temperature during the initial resting phase was 23°C . Taken together, these results demonstrated the ability of the virtual rat to capture the additive nature of heat stress as a combination of external environmental conditions and strenuous exercise.

To decouple the effects of environmental conditions and exercise on animal temperature, we performed additional sim-

ulations where we exclusively emulated the environmental conditions. For example, to account for only the environmental component of heat stress in *condition I*, we simulated thermal responses in the rat placed at an initial external temperature of 23°C for 30 min, followed by exposure to 33°C for 32 min, and finally cooled at 23°C , while at rest for each of the three phases. Figure 3*D* shows the comparison of the simulated maximum core temperatures in rats subjected to exercise at the various environmental conditions vs. simulated maximum core temperatures in rats not subjected to exercise for the same environmental conditions. We observed that for *condition I*, which involved a lower external temperature (33°C) than the other cases (38°C), heat stress due to exertion was dominant, with environmental conditions (no exercise) accounting for only 34% of the temperature rise from the initial, nonstress condition (Fig. 3*D*). For *condition II*, the environmental conditions accounted for 50% of the temperature rise, indicating an equal contribution of the high external temperature (38°C) and the exercise in the heat-stress response. Because of the extended exposure to a high external temperature (50 min at 38°C , as shown in Fig. 3*C*), heat stress due to the environmental conditions was dominant, accounting for 61% of the temperature rise for *condition III* (Fig. 3*D*). Figure 3*E* shows the computed spatial temperature distribution inside the rat body for *condition III*, which demonstrated noticeably higher temperatures during exercise compared with the no-exercise case.

Effect of exercise intensity on exertional heat stress. To investigate the effects of exercise intensity on heat stress, we used the protocol proposed by Walters et al. (27), which monitored brain temperatures in rats during exercise on a

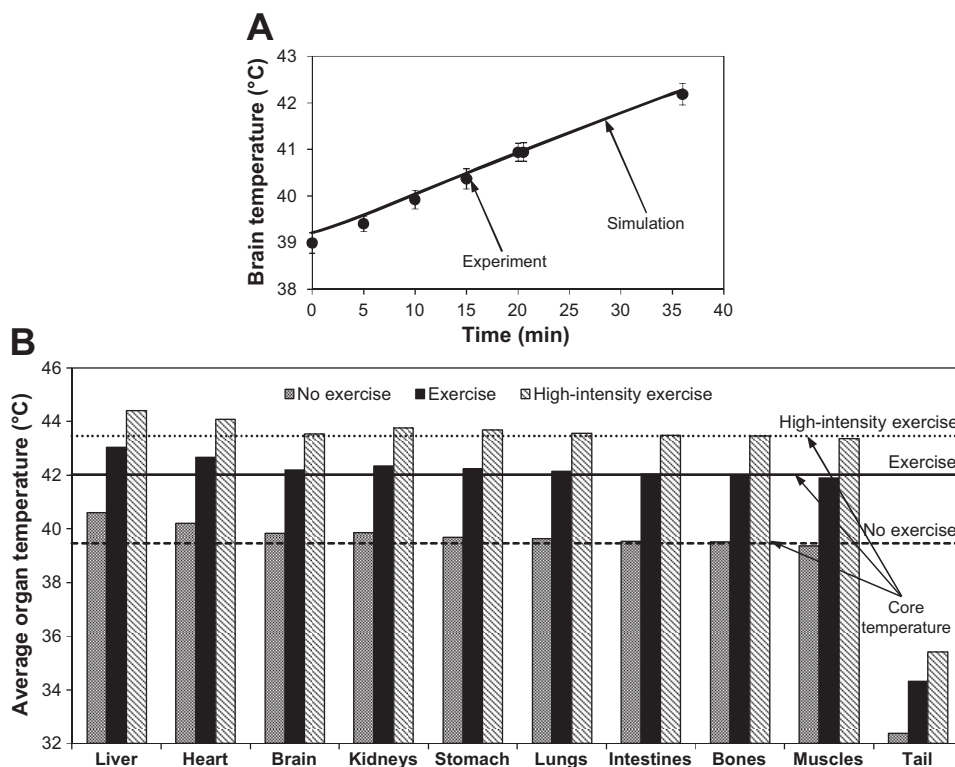
treadmill. This protocol allowed us to investigate the sole effect of exercise intensity on exertional heat stress without the confounding factors of different environmental temperatures (Fig. 3). In Walters et al. (27), rats first rested at a room temperature of 21°C for 60 min and then exercised at a treadmill speed of 18 m/min for 36 min at 35°C. Based on Eq. 1, the running speed corresponded to an exercise intensity of 75% of $\dot{V}O_{2\max}$ for untrained rats. First, we used the virtual rat to simulate exertional heat stress replicating these exercise conditions. Next, we increased the exercise intensity to 100% of $\dot{V}O_{2\max}$ and repeated the simulations. To facilitate comparisons, we also simulated a baseline case corresponding to no exercise.

Figure 4A shows the comparison of the predicted and experimentally measured brain temperatures. The simulation predicted a 3.1°C rise in brain temperature compared with the measured temperature increase of 3.2°C. Figure 4B shows the comparison of core and average organ temperatures for different exercise intensities at the end of the 36-min treadmill exercise. The core temperature increased by 2.6°C from a no-exercise condition (rest at 35°C external temperature) to an exercise intensity of 75% of $\dot{V}O_{2\max}$. For an additional 25% increase in exercise intensity (from 75% of $\dot{V}O_{2\max}$ to 100% of $\dot{V}O_{2\max}$), the core temperature increased by another 1.5°C. As with environmental heat stress (Fig. 2), the organs exhibited a differential thermal response for the different exercise intensities considered here, with the liver attaining the highest temperature for each case. The average liver temperature was 0.9 to 1.2°C higher than the core temperature for the three conditions. Similarly, average temperatures in the heart, brain, and kidneys were a maximum of 0.7, 0.4, and 0.4°C higher than the core temperature, respectively. Except for the tail, all other

organs were within 0.2°C of the core temperature for the three conditions.

Equivalent heat-stress response due to environmental conditions. We used simulations to determine the environmental condition that would elicit a thermal response in the rat equivalent to that observed during the exertional heat stress investigated immediately above. Starting from the same environmental condition (35°C) used in Ref. 27, we successively increased the external temperature, without subjecting the rat to exercise, until we obtained the same core temperature increase after 36 min as that observed for the exertional heat stress shown in Fig. 4A. We found that an external temperature of 50.5°C evoked the same core temperature response as that observed for the animal exercising at an intensity of 75% of $\dot{V}O_{2\max}$ at an external temperature of 35°C (Fig. 4A). Figure 5A shows a comparison of the spatial temperature distribution for the two cases. Although the core temperatures were constrained to be the same, the spatial temperature distributions were distinct for the two cases. Equivalent heat stress solely due to environmental conditions resulted in a significantly higher tail temperature compared with the exertional heat-stress case. A quantitative comparison of the minimum temperature (observed in the skin near the belly) and maximum temperature (observed in the tail) in the entire rat for the two cases showed that equivalent heat stress solely due to the environmental condition resulted in more uniform heating, with the minimum and maximum temperature values being closer (Fig. 5B). However, further investigation of the average organ temperatures for the two cases showed that the organ temperatures for the equivalent heat-stress case were within 0.2°C of the corresponding organ temperatures for the exertional heat-stress case. (Results are not shown because the

Fig. 4. Simulation of exertional heat stress in rats exercising at different intensities under the same external temperature based on the protocol used in Ref. 27. The experimental study consisted of measuring brain temperatures in male Sprague-Dawley rats ($n = 11$; 380–390 g) using a thermistor (Vitek; bio-Mérieux, Marcy l’Etoile, France) inserted into a stereotaxically implanted guide cannula (Vialon; Becton Dickinson, Franklin Lakes, NJ). A: comparison of simulation predictions and experimentally measured brain temperatures. Experimental data are shown as average values (dots) and standard error (vertical bars) ($n = 11$). B: simulated average temperature in key organs of rats exercising at different intensities: at rest, at 75% of maximal O_2 consumption ($\dot{V}O_{2\max}$), and at 100% of $\dot{V}O_{2\max}$ (high-intensity exercise).



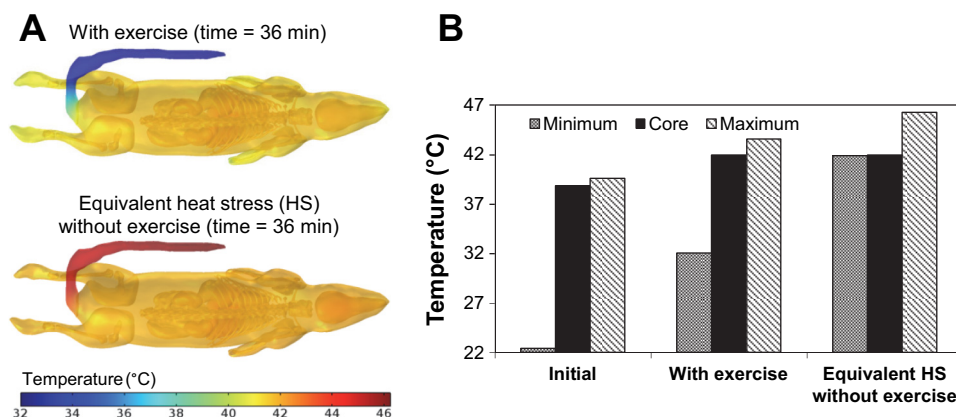


Fig. 5. Equivalent exertional-heat-stress response solely due to environmental conditions. *A*: comparison of the computed spatial temperature distribution in a rat subjected to exercise at an external temperature of 35°C with that of a rat subjected to a higher external temperature (50.5°C) without exercise (equivalent heat stress) to match the core temperature response. *B*: corresponding minimum, maximum, and core temperatures in the body for the 2 cases compared with their initial values (environmental temperature of 21°C) before being subjected to heat stress.

variations in organ temperatures between the two cases were insignificant.)

Effect of circadian rhythms on the heat-stress response. Next, to investigate the effects of circadian rhythms on the heat-stress response, we performed simulations to compute the spatiotemporal temperature distributions in rats exposed to the same heat-stress conditions at different times of the day. In our previous work (21), we showed the capability of the virtual rat to account for the circadian rhythmicity in core temperatures during an increase in the external temperature from 22 to 37°C over 163 min. Here, we repeated this simulation six times, starting the temperature increase at 0400, 0800 (as in Ref. 21), 1200, 1600, 2000, and 2400. Figure 6A shows the heating protocol for the two extreme cases (coolest and warmest) corresponding to heat stress starting at 1200 (*left*, the coolest) and 2400 (*right*, the warmest). We selected these two cases by comparing the core and organ temperatures from the six simulations.

Figure 6B shows the spatial temperature distribution after 2.75 h in rats subjected to heat stress starting at 1200 (*left*) and 2400 (*right*), indicating higher temperatures for the latter case. Figure 6C shows the average organ temperatures, which served to further quantify the differences in heat load in the different organs for the two cases. It also shows that the differences in maximum, minimum, and core temperatures in the animal between the two cases were 0.5, 0.2, and 0.6°C, respectively, demonstrating a differential thermal response for the same heat exposure at different times of the day. The core temperature difference (0.6°C) between the two cases was ~18% of the heat-stress-induced core temperature rise (3.4°C), which represents a significant variability in temperature response for the same experiment performed at different times of the day. We also observed a differential thermal response in the organs, with the difference in the average organ temperatures between the two cases ranging from 0.2°C in the tail to 0.8°C in the lungs. Other organs, including the liver, heart, brain, kidneys, stomach, and intestines, showed a difference of at least 0.5°C between the two cases. When we compared the heat-stress responses between 0800 and 1200, simulating experiments starting at early morning and midday, respectively, the core temperature difference was 0.5°C and the maximum organ temperature difference (in the stomach) was 0.7°C.

Whole body cooling for heat stress management. Finally, we investigated the effects of whole body cooling in rats after heat stress. To this end, we used the same protocol proposed by Yang et al. (29) described above (Fig. 2), where they moni-

tored the core temperature of rats undergoing heat stress. Here, post-heat stress, they cooled the animals at an external temperature of 16°C for 20 min before returning them to a normal ambient temperature of 26°C (Fig. 7A). Figure 7B shows that the temporal variations in the predicted core temperature profiles were consistent with the experimental results, both yielding a ~6.0°C core-temperature increase at the end of heat-stress exposure and a ~3.0°C temperature drop after whole body cooling. Figure 7C shows the spatial temperature distribution in the rat immediately after heat stress (time = 94 min) and after whole body cooling (time = 120 min). Although temperatures throughout the body decreased due to whole body cooling at 16°C, they did not return to normothermia. Similar to the observation during heating, the temperature drop was more pronounced in the tail than other parts of the body.

To investigate whether lowering the external cooling temperature would have a more profound effect on reducing body temperatures and achieve normothermia, we simulated the thermal response in the rat for a range of cooling temperatures. Figure 7D shows the differences in average temperatures between normothermia (before heat stress, external temperature of 26°C) and post-whole body cooling in various organs after 120 min at cooling temperatures of 16, 6, and 1°C, for 20 min. As a reference, we also plotted the average temperature difference for rats cooled at a room temperature of 26°C. After 20 min of cooling at room temperature (26°C), average temperatures in the internal organs were still elevated between 5.7 and 5.9°C above their normothermic values. We observed that with the application of successively lower external temperatures, the average organ temperature difference decreased, i.e., the organs moved toward normothermia, as expected. However, even after whole body cooling for 20 min at a significantly lower temperature (1°C), the organs did not return to the temperatures observed before heat stress; average temperatures in the internal organs were still elevated by 2.3 to 2.5°C above their normothermic values (Fig. 7D). Additional simulations showed that cooling times of 52 min at 16°C, 37 min at 6°C, and 32 min at 1°C would be required to return the core temperature to normothermic levels (before heat stress). An interesting observation from the simulations was that, although the internal organs remained at elevated temperatures after cooling for 20 min, the temperature in the tail decreased significantly, reaching hypothermic levels after cooling at 16, 6, and 1°C. For example, while the average tail temperature after cooling at room temperature (26°C) was still elevated by

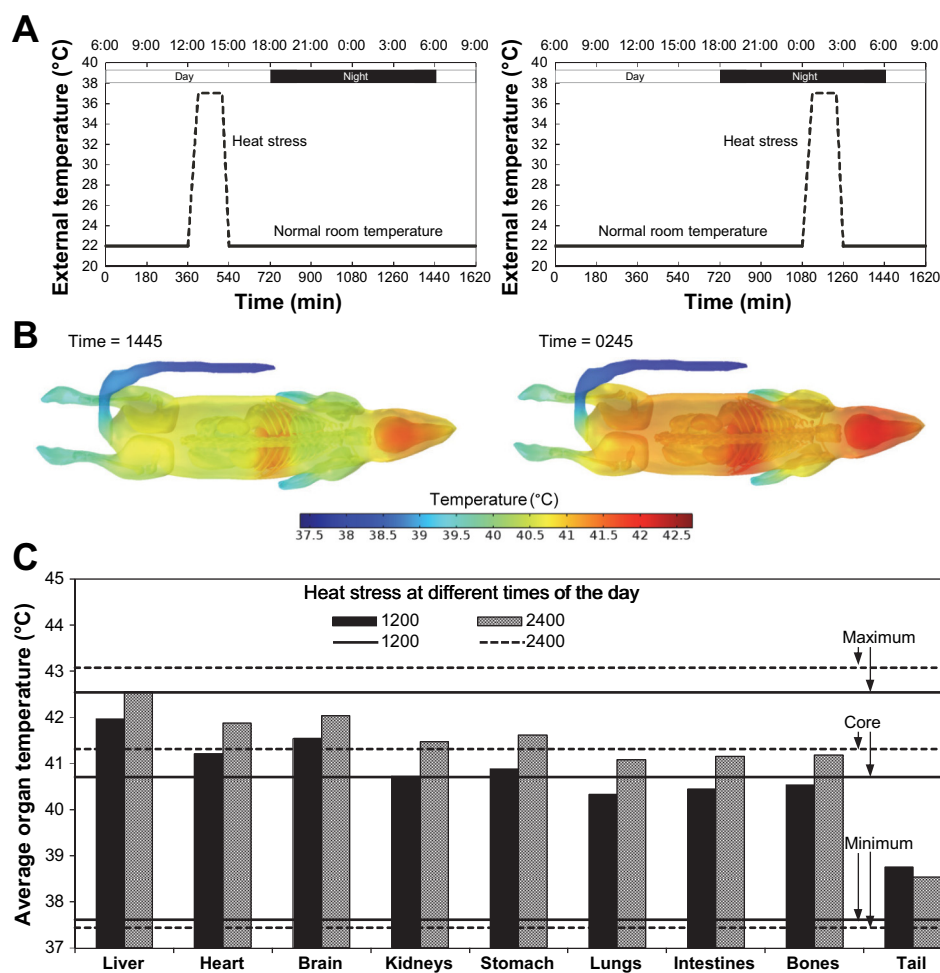


Fig. 6. Effect of circadian rhythms on the thermal response during heat stress based on the protocol proposed in our previous work (21). Shown are the results for the 2 extreme cases (coolest and warmest) selected out of 6 simulations of heat stress starting at different times during the day (0400, 0800, 1200, 1600, 2000, and 2400). *A*: external temperature profiles used to induce heat stress for these 2 cases [starting at 1200 (*left*) and starting at 2400 (*right*)]. *B*: comparison of the spatial temperature distribution in the rats for the 2 cases. *C*: comparison of the average organ, core, and extreme temperatures for the 2 cases.

3.2°C, after cooling at 16°C for 20 min, the tail temperature was 2.1°C lower than the normothermic tail temperature.

DISCUSSION

In our previous work, we presented a detailed three-dimensional computational model of a rat for predicting the spatio-temporal temperature distribution responses due to heat stress and validated it for one particular environmental heat-stress condition (21). Here, we substantially extended the validation of our model by using it to simulate four distinct heat-stress experimental studies induced by both elevated environmental temperature and exercise. We showed that, throughout all simulations, the predictions were within 0.6°C of the experimental measurements. Once validated, we used our “virtual rat” to investigate other conditions for which experimental data were not available. This allowed us to gain insights about whole animal, organ-specific thermal responses for different heat-stress and cooling scenarios, to compare and contrast the relative contributions of environmental conditions and exercise to heat stress, and to determine the effect of circadian rhythms on the temperature response. Importantly, the virtual rat allowed us to gain such insights, which may not be practical or possible to attain experimentally, without performing any additional animal studies.

A key finding from the simulations of heat stress under different environmental conditions was that the liver consis-

tently reached a higher temperature than the core and other organs (Figs. 2*D*, 4*B*, and 7*D*). This is corroborated by previous studies that reported liver damage due to severe heat stress in both rats (4) and humans (15). The heart reached the second-highest temperatures for the different environmental conditions. Note that core temperature is the temperature at a specific location and it should not be considered as the average temperature of the whole animal, which is affected by the significantly lower temperatures in the tail. Knowing these organ-specific temperature loads for different environmental conditions would allow for an improved understanding of heat injury progression to organ dysfunction.

Exertional heat stress is a particularly complicated condition to study experimentally using animal models (16, 27), because it is difficult to decouple the contribution of environmental factors from that of strenuous exercise. Moreover, it is time consuming and labor intensive to experimentally investigate a variety of exercise conditions, including a range of exercise intensities for both trained and untrained rats (14). In contrast, our virtual rat allowed us to investigate many distinct conditions by simply changing the model inputs and, importantly, to decouple the temperature response due to environmental conditions from the response due to physical activity.

The exertional heat-stress simulations provided a number of interesting results. First, we found that even if the rat exercised at a moderate intensity (68% of $\dot{V}O_{2max}$) and the room temper-

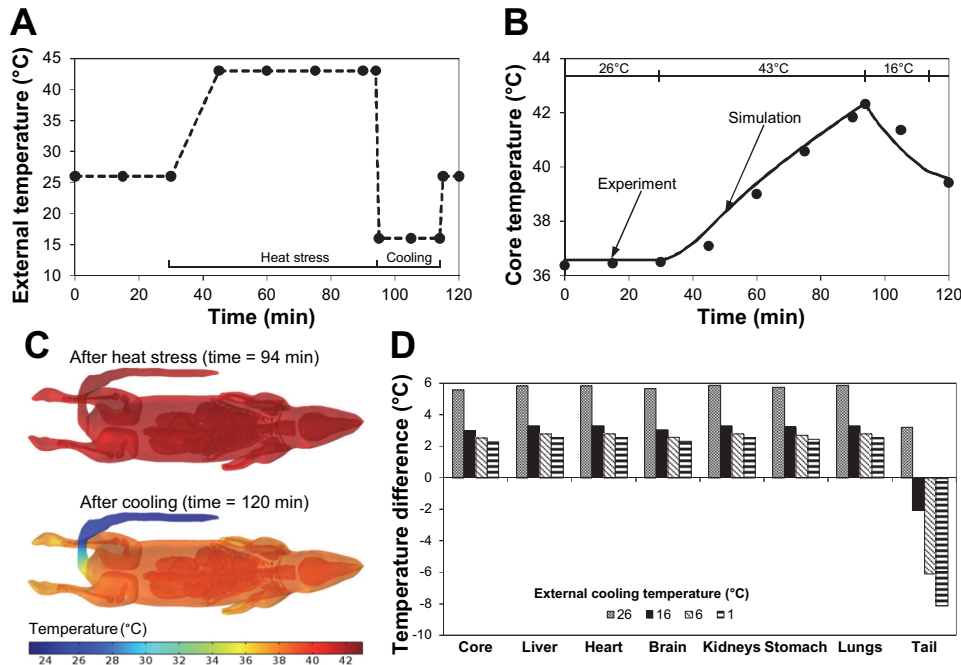


Fig. 7. Whole body cooling strategies for the protocol used in Ref. 29. The experimental study consisted of measuring core temperatures in adult male Sprague-Dawley rats ($n = 8$) weighing 238–312 g using a thermocouple (DR130; Yokogawa) inserted into the rectum during the heat-stress and cooling period. **A**: external temperature profile used to induce heat stress and subsequent cooling. **B**: comparison of predicted and measured core temperatures ($n = 8$). The dots (experimental data) represent the average values (standard errors were negligible). **C**: computed spatial temperature distribution immediately after heat stress (time = 94 min) and after cooling (time = 120 min). **D**: average organ and core temperature difference between nonstress conditions (external temperature of 26°C) and post whole body cooling at 120 min, after 20 min at 26, 16, 6, and 1°C.

ature (23°C) was increased by 10°C, exercise was still the dominant cause of heat stress (Fig. 3D). However, for a 15°C increase in the room temperature, the contributions from exercise and external temperature were equal. Finally, if rats were preheated at a high external temperature (38°C) for 30 min before exercise, the environmental condition was found to be the dominant heat-stress mechanism. Taken together, these observations provide important insights for the design of exertional heat-stress experiments. In the experimental study corresponding to these simulations, Fuller et al. (9) reported that the animals fatigued before they reached fatal temperatures. Therefore, for studies attempting to investigate the lethality associated with exertional heat stress, it may be important to preheat the animal before starting the exercise regimen (to increase body temperatures while limiting exercise) rather than inducing heat stress by subjecting the animal to high external temperature and exercise simultaneously.

The simulations also provided information about the organ-specific temperature response during exertional heat stress, which was previously unavailable. We found that, as with environmental heat stress, the liver demonstrated the highest temperatures for different exercise intensities (Fig. 4B), which is consistent with a previously reported observation of liver damage during exertional heat stress (10). Moreover, increasing the exercise intensity from moderate (75% of $\dot{V}O_{2max}$) to high (100% of $\dot{V}O_{2max}$) resulted in a significant increase (1.5°C) in the core temperature. Finally, to quantify the severity of exercise in terms of environmental conditions, we performed a unique simulation to determine the external temperature that would evoke the same core temperature response as that from exercise. We found that exercise at a moderate intensity level (75% of $\dot{V}O_{2max}$) and a moderately high temperature (35°C) yielded the same core temperature as that obtained by a resting animal at an extremely high external temperature (50.5°C). We also found that organ temperatures were similar for the two cases, except for the tail, implying that

heat stress under extremely high temperatures can be used as a surrogate for studying exertional heat stress in animal models if the main objective is to replicate the thermal response.

Simulations with the virtual rat also allowed us to quantify the effects of circadian rhythms on the thermal response during heat stress, which has not been experimentally studied. We found that there could be considerable differences (as large as 0.8°C) in the organ temperatures for heat stress induced at different times during the day for the same heating conditions (Fig. 6C). The simulation of whole body cooling using the virtual rat showed that it was not possible to reduce elevated body temperatures below a certain level in a short 20-min duration, even when using extreme cooling temperatures (16, 6, or 1°C; Fig. 7D). Reduction in external cooling temperature (as low as 1°C) only resulted in decreased tail temperatures but did not reduce the temperatures of the major organs significantly. Extremely low external temperatures are not desirable during whole body cooling, as they may lead to adverse hypothermic effects, including cardiovascular and pulmonary complications due to hypotension, pneumonia, aneurysms, or thrombocytopenia (6). Therefore, localized cooling strategies targeting specific organs that reach the highest temperatures (such as the liver, heart, and brain) could be more effective than whole body cooling. We also demonstrated how simulations could be potentially used to design cooling experiments and strategies by determining the conditions needed to achieve normothermia.

Although we compared the model predictions with published experimental data wherever possible, we could not validate the model-predicted temperatures for all organs and their circadian variations during heat stress and whole body cooling due to the unavailability of experimental data. Moreover, similar to previous modeling efforts (12, 13, 23, 26), it was not possible to account for different rat strains in our simulations because of the unavailability of a complete set of model parameters for any particular rat strain. In addition, we could not incorporate the effects of animal weight and size on

the temperature response, which would require acquisition of medical images and three-dimensional anatomy reconstruction for each animal. Therefore, for model development, we used physiological data from various rat strains and anatomical data from one representative rat. As such, the model represents the heat transfer processes of an “average” rat. The good agreements between model predictions and experimental measurements seem to indicate that such simplifications are justifiable for the conditions studied here.

In summary, we used a unifying framework based on computational modeling to investigate different aspects of heat stress. The value of this approach is that it provides the means to gain new insights into previous heat-stress studies beyond what is feasible through animal experimentation alone. This, in turn, not only enabled us to develop greater insights into various heat-stress scenarios but can also help to reduce the number of animals used in experiments. We demonstrated that once the simulations are validated for particular heat-stress conditions, other relevant heat-stress episodes can be simulated using our virtual rat. Customized experiments can potentially be designed based on such simulations, thereby reducing the number of animals used for experimentation. Furthermore, the unique insights obtained from our results can be used to better understand organ-specific disorders observed during heat stress and to develop optimized heat-stress management techniques.

Software availability. The virtual rat model is publicly available upon request to users who have purchased a license for the third-party geometry (ROBY, Duke University, Durham, NC) used in our model. To request the model, please visit <http://bhsai.org/software>. For information on the ROBY license, please contact Dr. W. Paul Segars (paul.segars@duke.edu).

ACKNOWLEDGMENTS

We thank Dr. Patrick A. Mason (Office of the Director of Assistant Secretary of Defense for Research and Engineering), Dr. John Ziriaux (Naval Surface Warfare Center Dahlgren Division), and Dr. W. Paul Segars (Duke University Medical Center) for sharing the initial rat anatomical models.

GRANTS

The research was supported by the U.S. Army Network Science Initiative and the Military Operational Medicine Research Program, U.S. Army Medical Research and Materiel Command, Fort Detrick, MD.

DISCLAIMER

The opinions and assertions contained herein are the private views of the authors and are not to be construed as official or as reflecting the views of the U.S. Army or of the U.S. Department of Defense. This paper has been approved for public release with unlimited distribution.

DISCLOSURES

No conflicts of interest, financial or otherwise, are declared by the author(s).

AUTHOR CONTRIBUTIONS

Author contributions: V.R., J.D.S., and J.R. conception and design of research; V.R. performed experiments; V.R. analyzed data; V.R. and J.R. interpreted results of experiments; V.R. prepared figures; V.R. drafted manuscript; V.R., J.D.S., and J.R. edited and revised manuscript; V.R., J.D.S., and J.R. approved final version of manuscript.

REFERENCES

1. **Armed Forces Health Surveillance Center.** *Heat Injuries, Active Component, US Armed Forces, 2011 Medical Surveillance Monthly Report (MSMR)*. Silver Spring, MD: Armed Forces Health Surveillance Center, 2012, vol. 19, p. 14–16, 2012.
2. **Armstrong LE, Casa DJ, Millard-Stafford M, Moran DS, Pyne SW, Roberts WO.** American College of Sports Medicine position stand. Exertional heat illness during training and competition. *Med Sci Sports Exerc* 39: 556–572, 2007.
3. **Bouchama A, Knochel JP.** Heat stroke. *N Engl J Med* 346: 1978–1988, 2002.
4. **Bowers WD, Jr., Hubbard RW, Leav I, Daum R, Conlon M, Hamlet MP, Mager M, Brandt P.** Alterations of rat liver subsequent to heat overload. *Arch Pathol Lab Med* 102: 154–157, 1978.
5. **Brotherhood JR.** Heat stress and strain in exercise and sport. *J Sci Med Sport* 11: 6–19, 2008.
6. **Christian E, Zada G, Sung G, Giannotta SL.** A review of selective hypothermia in the management of traumatic brain injury. *Neurosurg Focus* 25: E9, 2008.
7. **Damanhoury ZA, Tayeb OS.** Animal models for heat stroke studies. *J Pharmacol Toxicol Methods* 28: 119–127, 1992.
8. **Epstein Y, Roberts WO.** The pathophysiology of heat stroke: an integrative view of the final common pathway. *Scand J Med Sci Sports* 21: 742–748, 2011.
9. **Fuller A, Carter RN, Mitchell D.** Brain and abdominal temperatures at fatigue in rats exercising in the heat. *J Appl Physiol* 84: 877–883, 1998.
10. **Giercksky T, Boberg KM, Farstad IN, Halvorsen S, Schrumph E.** Severe liver failure in exertional heat stroke. *Scand J Gastroenterol* 34: 824–827, 1999.
11. **Gordon CJ.** *Temperature Regulation in Laboratory Rodents*. Cambridge, UK: Cambridge Univ. Press, 1993, p. 16–17.
12. **Grosman B, Shaik OS, Helwig BG, Leon LR, Doyle FJ 3rd.** A physiological systems approach to modeling and resetting of mouse thermoregulation under heat stress. *J Appl Physiol* 111: 938–945, 2011.
13. **Hirata A, Masuda H, Kanai Y, Asai R, Fujiwara O, Arima T, Kawai H, Watanabe S, Lagroye I, Veyret B.** Computational modeling of temperature elevation and thermoregulatory response in the brains of anesthetized rats locally exposed at 1.5 GHz. *Phys Med Biol* 56: 7639–7657, 2011.
14. **Hoydal MA, Wisloff U, Kemi OJ, Ellingsen O.** Running speed and maximal oxygen uptake in rats and mice: practical implications for exercise training. *Eur J Cardiovasc Prev Rehabil* 14: 753–760, 2007.
15. **Kew M, Bersohn I, Seftel H, Kent G.** Liver damage in heatstroke. *Am J Med* 49: 192–202, 1970.
16. **Leon LR.** Heat stroke and cytokines. *Prog Brain Res* 162: 481–524, 2007.
17. **Leon LR, Helwig BG.** Heat stroke: role of the systemic inflammatory response. *J Appl Physiol* 109: 1980–1988, 2010.
18. **Lu KC, Wang JY, Lin SH, Chu P, Lin YF.** Role of circulating cytokines and chemokines in exertional heatstroke. *Crit Care Med* 32: 399–403, 2004.
19. **Patch LD, Brooks GA.** Effects of training on $\dot{V}O_{2\max}$ and $\dot{V}O_2$ during two running intensities in rats. *Pflügers Arch* 386: 215–219, 1980.
20. **Pennes HH.** Analysis of tissue and arterial blood temperatures in the resting human forearm. *J Appl Physiol* 1: 93–122, 1948.
21. **Rakesh V, Stallings JD, Helwig BG, Leon LR, Jackson DA, Reifman J.** A 3-D mathematical model to identify organ-specific risks in rats during thermal stress. *J Appl Physiol* 115: 1822–1837, 2013.
22. **Refinetti R.** Metabolic heat production, heat loss and the circadian rhythm of body temperature in the rat. *Exp Physiol* 88: 423–429, 2003.
23. **Samaras T, Regli P, Kuster N.** Electromagnetic and heat transfer computations for non-ionizing radiation dosimetry. *Phys Med Biol* 45: 2233–2246, 2000.
24. **Shido O, Nagasaka T.** Thermoregulatory responses to acute body heating in rats acclimated to continuous heat exposure. *J Appl Physiol* 68: 59–65, 1990.
25. **Shido O, Sakurada S, Kohda W, Nagasaka T.** Day-night changes of body temperature and feeding activity in heat-acclimated rats. *Physiol Behav* 55: 935–939, 1994.
26. **Trakic A, Crozier S, Liu F.** Numerical modelling of thermal effects in rats due to high-field magnetic resonance imaging (0.5–1 GHz). *Phys Med Biol* 49: 5547–5558, 2004.
27. **Walters TJ, Ryan KL, Tate LM, Mason PA.** Exercise in the heat is limited by a critical internal temperature. *J Appl Physiol* 89: 799–806, 2000.
28. **Wissler EH.** Pennes’ 1948 paper revisited. *J Appl Physiol* 85: 35–41, 1998.
29. **Yang HH, Chang CP, Cheng RT, Lin MT.** Attenuation of acute lung inflammation and injury by whole body cooling in a rat heatstroke model. *J Biomed Biotechnol* 2009: 768086, 2009.